Atrial Fibrillation in Acute Obstructive Sleep Apnea: Autonomic Nervous Mechanism and Modulation

Lilei Yu, MD, PhD;* Xuefei Li, MD;* Bing Huang, MD, PhD; Xiaoya Zhou, MD, PhD; Menglong Wang, MD; Liping Zhou, MD; Guannan Meng, MD; Yuhong Wang, MD; Zhenya Wang, MD; Jielin Deng, MD; Hong Jiang, MD, FACC

Background—The mechanisms of atrial fibrillation (AF) induced by obstructive sleep apnea (OSA) are not completely understood. This study investigated the roles of the intrinsic and extrinsic cardiac autonomic nervous system in OSA-induced AF and provided noninvasive autonomic nervous modulation for the suppression of OSA-induced AF by using low-level transcutaneous electrical stimulation (LL-TS) of the auricular branch of the vagus nerve at the tragus.

Methods and Results—Eighteen dogs received tracheostomy under general anesthesia and were randomly divided into 3 groups: the OSA group (OSA was simulated via clamping of the endotracheal tube at end expiration for 1.5 minutes every 10 minutes, n=6), the LL-TS + OSA group (simulated OSA plus LL-TS, at 80% of the slowing sinus rate, n=6), and the control group (sham surgery without stimulation, n=6). The effective refractory period was significantly shortened after 1 hour of simulated OSA, and the window of vulnerability and plasma norepinephrine levels were both markedly increased in the OSA group. OSA dramatically increased the neural function and activity of the intrinsic and extrinsic cardiac autonomic nervous system, including the superior left ganglionated plexus, the left stellate ganglion, and the left renal sympathetic nerve. OSA also significantly upregulated the expression levels of c-fos and nerve growth factor in the superior left ganglionated plexus and the left stellate ganglion. However, LL-TS markedly improved these parameters.

Conclusions—These findings suggest that the intrinsic and extrinsic cardiac autonomic nervous system plays crucial roles in the acute stage of OSA-induced AF. Noninvasive LL-TS suppressed shortening of atrial refractoriness and autonomic remodeling, which prevented OSA-induced AF. (*J Am Heart Assoc*. 2017;6:e006264. DOI: 10.1161/JAHA.117.006264.)

Key Words: atrial fibrillation • autonomic nervous system • obstructive sleep apnea • tragus stimulation

Obstructive sleep apnea (OSA) is one of the most common forms of sleep-disordered breathing, and it is highly associated with atrial fibrillation (AF).[1–4] OSA can shorten the atrial effective refractory period (ERP) and increase the inducibility of AF, which are strong triggers for AF.[5,6] Previous studies focused on the electrophysiological,[5]

From the Department of Cardiology, Renmin Hospital of Wuhan University, Wuhan, Hubei, China (L.Y., X.L., B.H., X.Z., M.W., L.Z., G.M., Y.W., Z.W., J.D., H.J.); Cardiovascular Research Institute, Wuhan University, Wuhan, Hubei, China (L.Y., X.L., B.H., X.Z., M.W., L.Z., G.M., Y.W., Z.W., J.D., H.J.); Hubei Key Laboratory of Cardiology, Wuhan, Hubei, China (L.Y., X.L., B.H., X.Z., M.W., L.Z., G.M., Y.W., Z.W., J.D., H.J.).

*Dr Yu and Dr Li contributed equally to this work.

Correspondence to: Hong Jiang, MD, FACC and Lilei Yu, MD, PhD, Department of Cardiology, Renmin Hospital of Wuhan University, No. 238 Jiefang Road, Wuchang District, Wuhan, Hubei 430060, China. E-mails: whujianghong@163.com; whuyulilei@163.com

sympathovagal,[7–9] and neurohumoral[10] properties of OSA-induced AF. However, these studies did not conclusively define a mechanism.

OSA induces hyperactivity of the autonomic nervous system, which is an established contributing factor to AF.[11–13] The cardiac autonomic nervous system (CANS) could be basically divided into extrinsic and intrinsic CANS, based on the location of neural control of the heart.[14,15] Extrinsic CANS is composed of the soma in brain nuclei, vagosympathetic trunks, chains of ganglia along the spinal cord, and the postganglionic axons that course en route to the heart. Intrinsic CANS is composed of a neural network of axons and autonomic ganglia concentrated at the ganglionated plexi within the pericardium. A previous study showed hyperactivity at the ganglionated plexi (intrinsic CANS) during OSA, and ganglionated plexi ablation markedly inhibited the OSA-induced atrial ERP shortening and AF inducibility.[7] Renal denervation is an effective approach to reducing sympathetic activity, and it suppressed OSA-induced AF.[5,10] Our recent study demonstrated that stimulation of the renal sympathetic nerve (RSN; extrinsic CANS) facilitated AF.[16] Previous studies indicated that hyperactivity of the left stellate ganglion (LSG;

Clinical Perspective

What Is New?

- This study is the first to demonstrate that hyperactivity of the intrinsic and extrinsic cardiac autonomic nervous system plays crucial roles in the acute stage of obstructive sleep apnea–induced atrial fibrillation.
- Low-level transcutaneous electrical stimulation of the auricular branch of the vagus nerve at the tragus, a noninvasive autonomic modulation, suppresses shortening of atrial refractoriness and hyperactivity of the intrinsic and extrinsic cardiac autonomic nervous system, thereby preventing obstructive sleep apnea–induced atrial fibrillation.

What Are the Clinical Implications?

- Modulation of the intrinsic and extrinsic cardiac autonomic nervous system by low-level transcutaneous electrical stimulation might be a novel therapy for obstructive sleep apnea–induced atrial fibrillation.

extrinsic CANS) was highly associated with AF.[17,18] Consequently, we hypothesized that the intrinsic and extrinsic CANS, including the ganglionated plexi, LSG and RSN, plays key roles in the process of OSA-induced AF.

The present study used a canine model of simulated OSA to systematically investigate the roles of the intrinsic and extrinsic CANS in the process of OSA-induced AF and examined possible underlying mechanisms. We also developed a potential noninvasive approach for treating OSA-induced AF by using low-level transcutaneous electrical stimulation (LL-TS) of the auricular branch of the vagus nerve at the tragus to modulate the function of the intrinsic and extrinsic CANS.

Methods

All experimental protocols conformed to the Guideline for the Care and Use of Laboratory Animals published by the US National Institutes of Health, and the Committee on the Ethics of Animal Experiments of Wuhan University approved all protocols.

Animal Preparation

Eighteen adult male mongrel dogs (20±4 kg) were anesthetized via an intravenous injection of sodium pentobarbital 30 mg/kg. Anesthesia was maintained using 50 to 100 mg sodium pentobarbital every hour as needed. All animals were artificially ventilated using a cuffed endotracheal tube attached to a positive pressure respirator (tidal volume, 300 mL; respiratory rate, 20 breaths/min; level of FiO_2, 21%).

The left femoral artery and vein were cannulated to monitor arterial blood pressure (BP) and to deliver drug and saline infusions, respectively. Standard surface ECGs were consistently recorded using a computer-based Lab System (LEAD7000; Jinjiang Ltd) throughout the experiment. Bilateral thoracotomy was performed at the fourth intercostal space. Multielectrode catheters were sutured at the left and right superior pulmonary veins, left and right inferior pulmonary veins, left and right atrial appendage, and left and right atria.

Experiment Protocol

Eighteen dogs were randomly divided into 3 groups: the OSA group (OSA for 1 hour, n=6), the LL-TS + OSA group (1 hour of OSA plus 1 hour of LL-TS, n=6), and the control group (sham OSA without stimulation, n=6). Figure 1A outlines the protocol.

Establishment of the OSA Model

The OSA model was induced by clamping the proximal end of the endotracheal cannula at end expiration, as described previously.[7,8] Briefly, apnea was achieved by clamping the proximal end of the endotracheal cannula for 1.5 minutes, and the dog was ventilated for 8.5 minutes. This obstructive respiratory event was repeated every 10 minutes for 1 hour.

LL-TS Stimulation

Tragus stimulation (auricular branch of vagus nerve) in the left ear was accomplished using ear clips with electrodes connected to a custom-made stimulator (frequency 20 Hz, pulse width 1 ms, stimulation 5 seconds, interval 5 seconds), as described previously.[19,20] Briefly, incremental voltages were applied to the tragus until a slowing of the sinus rate or atrioventricular conduction was observed (measured as the atrioventricular interval). The voltage necessary to slow the sinus rate or atrioventricular conduction was defined as the threshold, and the intensity of LL-TS stimulation was set at 80% below the threshold.

Programmed Stimulation

ERP and AF inducibility were determined at baseline and 1 hour during the experiment. The ERP at atrium and pulmonary vein sites were determined using programmed stimulation that consisted of 8 consecutive stimuli (S1–S2=330 ms) and a premature stimuli (S1–S2) at 2 times the diastolic threshold. The S1 to S2 interval was decreased from 160 ms initially in decrements of 10 to 2 ms when approaching ERP. The window of vulnerability (WOV) was defined as the difference between the longest
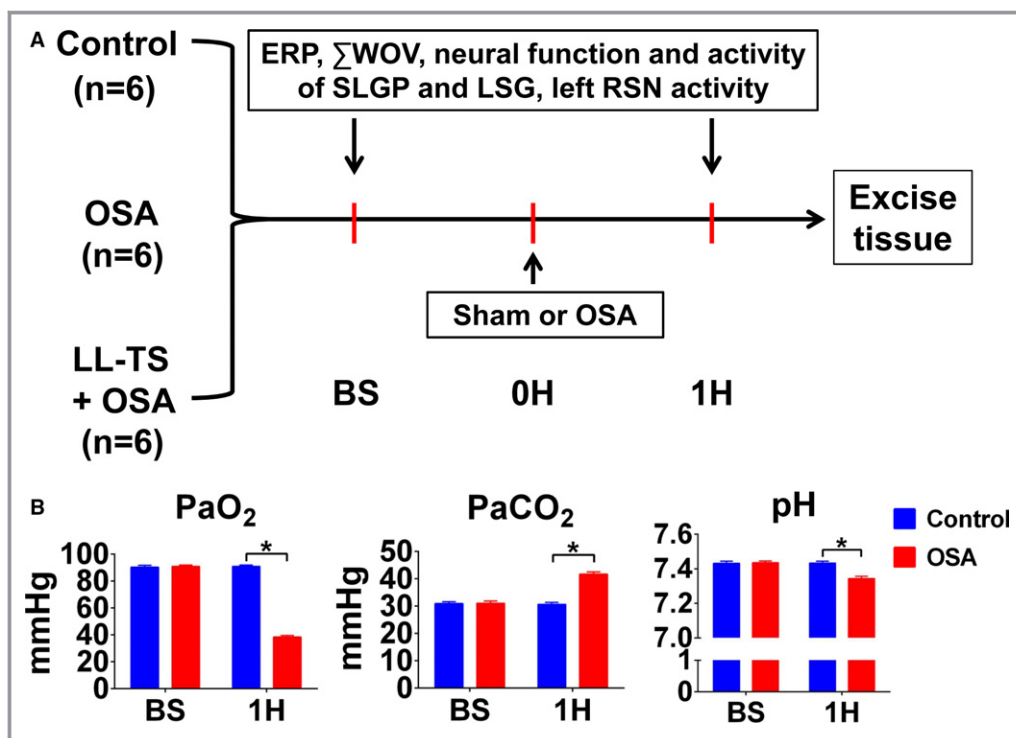
Figure 1. Study protocol (A) and changes in blood gases between the control group and the OSA group (n=6) (B). *$P<0.05$ vs the control group. BS indicates baseline; ERP, effective refractory period; LL-TS, low-level transcutaneous electrical stimulation; LSG, left stellate ganglion; OSA, obstructive sleep apnea; RSN, renal sympathetic nerve; ΣWOV, cumulative window of vulnerability; SLGP, superior left ganglionated plexus.

and shortest S1 to S2 interval at which AF was induced. The WOV was used as an index of AF inducibility.[19,21] The cumulative WOV (ΣWOV) was the sum of WOVs at all sites in each dog. AF was defined as irregular atrial beatings >500 beats/min.

Measurements of Neural Function and Activity

Superior left ganglionated plexi (SLGP) and LSG function were measured, as described previously.[16] Briefly, SLGP function was determined as the maximal change in sinus rate, and LSG function was measured as the maximal change in systolic BP in response to direct electrical stimulation of SLGP or LSG. High-frequency stimulation (20 Hz, 0.1-ms pulse duration) was applied to the SLGP or LSG using a Grass-S88 stimulator (Astro-Med). The SLGP and LSG exhibited significantly different responses to high-frequency stimulation in each dog. Consequently, we used incremental voltages to stimulate the SLGP and LSG (level 1: 1–4.9 V; level 2: 5–7.4 V; level 3: 7.5–9.9 V; level 4: 10–14.9 V; and level 5: 15–20 V) to equalize these differences. The voltage/sinus rate and voltage/BP response curves were constructed as described in previous studies.[16,18] Each high-frequency stimulation lasted <30 seconds.

Neural activities of SLGP, LSG, and left RSN were recorded, as described previously.[7,16,22,23] Briefly, the left renal nerves were exposed via a left flank incision and dissected free from surrounding tissue. Bipolar platinum recording microelectrodes were placed on one of the left renal nerves and covered with mineral oil when an optimal signal:noise ratio was achieved. Two tungsten-coated micro-electrodes were inserted into the SLGP or the LSG to record neural activity. The microelectrodes were mounted on a Powerlab data acquisition system (8/35; AD Instruments). Nerve signals were amplified using an amplifier (DP-304; Warner Instruments). The spike frequency and amplitude, defined as deflections with a signal:noise ratio >3:1, were used to quantitate neural activity.[24] A 1-minute recording of the SLGP, LSG, or left RSN neural activity during sinus rhythm was acquired immediately at baseline and 1 hour during the experiment.

Western Blot

SLGP and LSG tissues were excised at the end of the experiment, washed with saline, and stored at −80°C for later analyses. Protein expression levels of c-fos and neural growth factor (NGF) in SLGP and LSG were analyzed using western blot

analysis, as described previously.[16] Briefly, equal amounts of denatured protein were electrophoresed in a 10% SDS–polyacrylamide gel and transferred to a nitrocellulose membrane. Membranes were blocked with 5% nonfat dry milk for 2 hours and incubated with primary antibodies (c-fos and NGF) at 4°C overnight. Membranes were washed and incubated with secondary antibodies at 37°C for 2 hours. Protein bands were visualized using an enhanced chemiluminescence system, and β-actin was used as an internal control.

Immunofluorescence Staining

Immunofluorescence staining was used to confirm the expression and location of c-fos and NGF in the LSG. Paraffin-embedded LSG was cut transversely into 5-μm-thick sections. Sections were incubated in PBS containing 10% fetal bovine serum for 30 minutes and incubated overnight at 4°C with primary antibodies (c-fos, NGF, tyrosine hydroxylase). Sections were washed in PBS and incubated with secondary antibody for 1 hour at 37°C. Nuclei were stained with DAPI (4′,6-diamidino-2-phenylindole). All images were obtained using a fluorescence microscope (Olympus DX51) and DP2-BSW software 2.2 (Olympus) and analyzed using Image-Pro Plus 6.0 (Media Cybernetics).

Blood Sampling

Venous blood samples were collected from the jugular vein at baseline and 1 hour, and were centrifuged at 1000 g for 15 minutes. Supernatants were stored at −80°C for later analyses. ELISAs were used to measure the plasma levels of norepinephrine, according to the manufacturer's instruction (Elabscience).

Arterial blood for blood gas analysis was drawn from the femoral arterial sheath via an anaerobic heparinized syringe at baseline and 1.5 minutes after the last simulated OSA event. PaO_2, $PaCO_2$, and pH values were calculated using a VetScan i-STAT1 Analyzer (Abbott Point of Care Inc) within 5 minutes of collection.

Statistical Analyses

All continuous data are expressed as mean±SD and analyzed using SPSS 19.0 (IBM Corp). Two-way repeated-measures ANOVA was used to examine the effect of each intervention on the respective parameters over time, and the Bonferroni test was used for post hoc multiple comparisons. A 1-way ANOVA followed by the Bonferroni post hoc test was used for multiple comparisons of c-fos and NGF between groups. All plotting graphics were created using the GraphPad Prism 6.0 software. $P<0.05$ were considered statistically significant.

Results

Blood Gases

Figure 1B shows that blood analyses of PaO_2, $PaCO_2$, and pH at baseline were not significantly different between the control and OSA groups ($P>0.05$). However, substantial decreases in the levels of PaO_2 (90.9±1.0 versus 38.4±1.2 mm Hg, $P<0.05$) and pH (7.44±0.01 versus 7.34±0.01, $P<0.05$) and a significant increase in $PaCO_2$ (31.1±0.8 versus 41.7±0.9 mm Hg, $P<0.05$) were observed in the OSA group after 1 hour of simulated OSA compared with the control group, which validated the OSA model.

ERP and ΣWOV

No significant differences in ERP and ΣWOV values were observed between groups at baseline ($P>0.05$). The ERP at all sites was significantly shortened after 1 hour of simulated OSA; the ΣWOV increased markedly in the OSA group compared with the control group, and LL-TS significantly inhibited this ERP shortening and increased ΣWOV (all $P<0.05$, Figure 2). For example, the ERP was not significantly different between groups at baseline at the right superior pulmonary vein site, and it was 120.0±6.3, 76.3±12.6, and 128.0±11.9 ms at 1 hour in the control, OSA, and LL-TS + OSA groups, respectively. The ΣWOV is an index of AF inducibility, and it was 1.7±2.7, 43.3±26.4, and 2.3±2.9 ms at 1 hour in the control, OSA, and LL-TS + OSA groups, respectively.

BP and Plasma Levels of Norepinephrine

No significant differences in systolic and diastolic BP were observed among the 3 groups at baseline ($P>0.05$). Systolic and diastolic BP increased markedly in the OSA group as a result of simulated OSA (systolic BP: 125.5±11.5 versus 183.0±22.1 mm Hg; diastolic BP: 90.0±23.2 versus 132.7±23.5 mm Hg, $P<0.05$) and in the LL-TS + OSA group (systolic BP: 180.5±22.8 mm Hg; diastolic BP: 138.3±27.6 mm Hg) compared with the control group, but no significant differences were observed between the OSA group and the LL-TS + OSA group ($P>0.05$; Figure 3A and 3B).

As shown in Figure 3C, the plasma levels of norepinephrine in the 3 groups were not significantly different at baseline. The plasma norepinephrine levels increased markedly in the OSA group after 1-hour simulated OSA (13.8±3.6 versus 21.8±9.5 ng/mL, $P<0.05$) compared with the control group, and LL-TS significantly decreased the increased plasma norepinephrine levels (14.6±4.3 ng/mL, $P<0.05$).
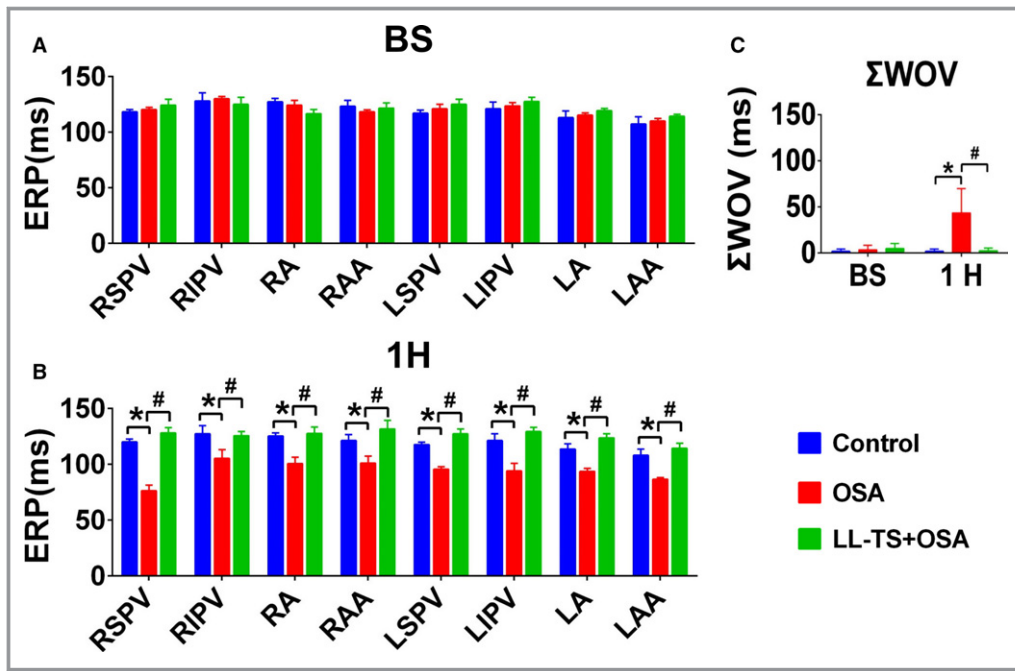
Figure 2. Changes in ERP and ΣWOV among the control, OSA, and LL-TS + OSA groups (n=6). A, ERP at baseline. (B) ERP at 1 hour. (C) ΣWOV in the 3 groups. *$P<0.05$ vs the control group; #$P<0.05$ vs the OSA group. BS indicates baseline; ERP, effective refractory period; LA, left atrium; LAA, left atrial appendage; LIPV, left inferior pulmonary vein; LL-TS, low-level transcutaneous electrical stimulation; LSPV, left superior pulmonary vein; OSA, obstructive sleep apnea; RA, right atrium; RAA, right atrial appendage; RIPV, right inferior pulmonary vein; RSPV, right superior pulmonary vein; ΣWOV, cumulative window of vulnerability.

Neural Function of SLGP and LSG

High-frequency stimulation of SLGP and LSG significantly slowed the sinus rate and increased systolic BP in the control, OSA, and LL-TS + OSA groups at baseline. The abilities of the SLGP to slow the sinus rate and LSG to increase systolic BP after 1 hour of simulated OSA were significantly augmented at the same incremental voltage levels of SLGP and LSG stimulation in the OSA group, and LL-TS markedly inhibited the OSA-induced enhanced neural function of SLGP and LSG (all $P<0.05$; Figure 4). For example, the sinus rate–slowing and systolic BP–increasing response induced by high-frequency stimulation increased markedly in the OSA group at voltage level 4 compared with baseline (SLGP: $45.9\pm4.2\%$ versus $63.6\pm7.0\%$; LSG: $35.0\pm5.5\%$ versus $44.3\pm10.7\%$, $P<0.05$), and LL-TS produced no significant increase (SLGP: $42.7\pm6.1\%$ versus $48.1\pm11.0\%$; LSG: $35.0\pm5.1\%$ versus $38.1\pm4.5\%$; $P>0.05$) after 1-hour simulated OSA.
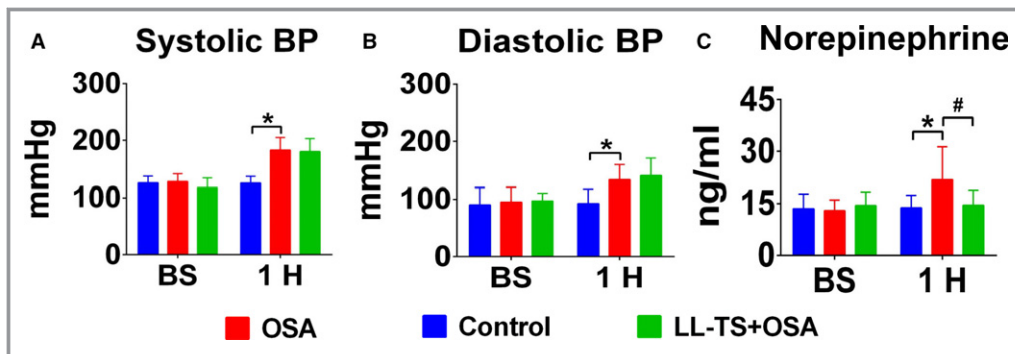

Figure 3. Changes in BP and norepinephrine plasma levels in the OSA (A), control (B), and LL-TS + OSA (C) groups (n=6). *$P<0.05$ vs the control group; #$P<0.05$ vs the OSA group. BP indicates blood pressure; BS, baseline; LL-TS, low-level transcutaneous electrical stimulation; OSA, obstructive sleep apnea.
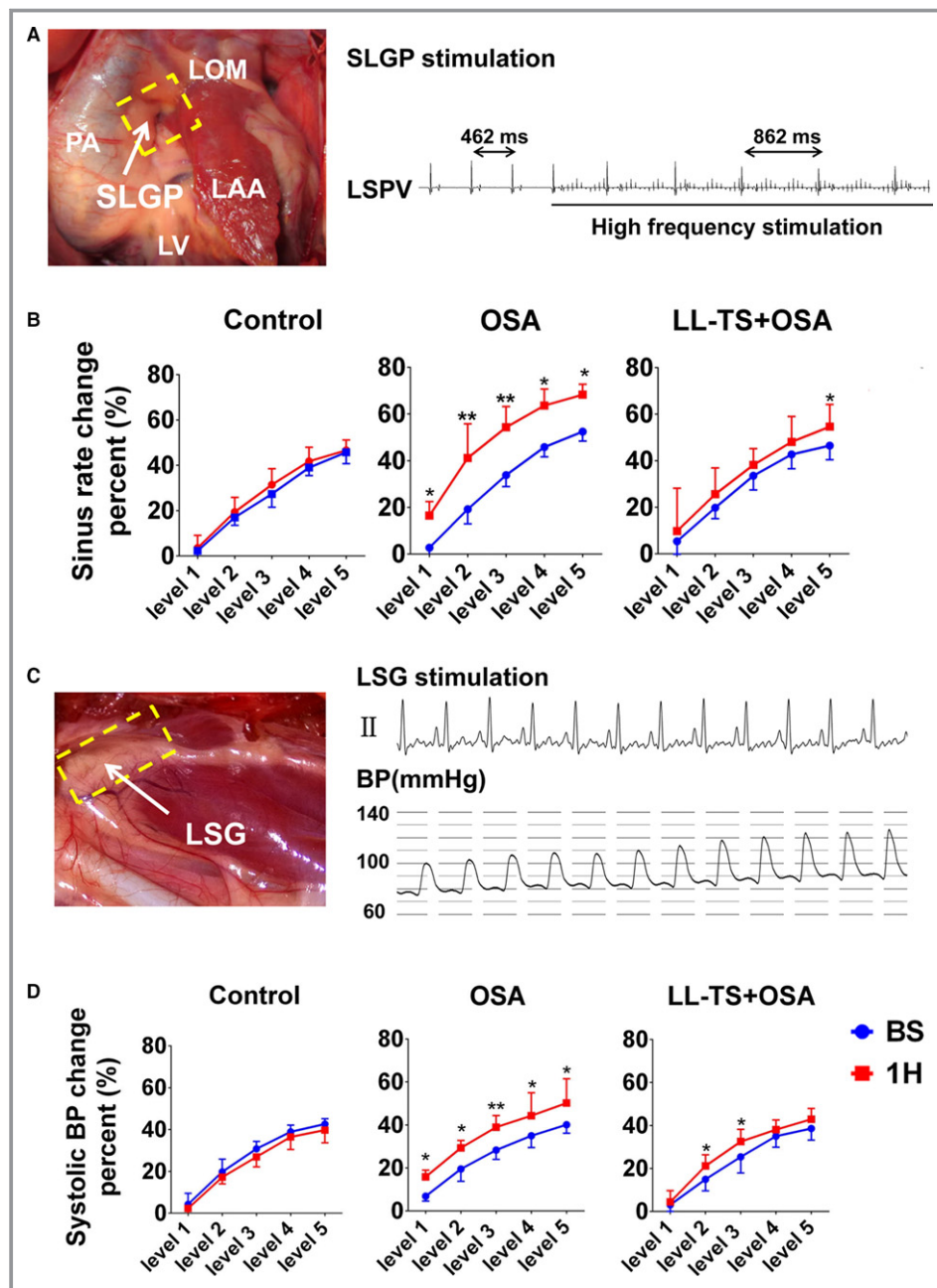
Figure 4. Autonomic neural function changes in the control, OSA, and LL-TS + OSA groups. A, The anatomical position of the SLGP and representative example of sinus rate–slowing response to SLGP stimulation. (B) Sinus rate–slowing response to the high-frequency stimulation of the SLGP across groups (n=6). (C) The anatomical position of the LSG and representative illustration of systolic BP–increasing response to LSG stimulation. (D) systolic BP–increasing response to the high-frequency stimulation of the LSG in the 3 groups (n=6). *$P<0.05$ vs the baseline, **$P<0.01$ vs the baseline. BP indicates blood pressure; BS, baseline; LAA, left atrial appendage; LL-TS, low-level transcutaneous electrical stimulation; LOM, ligament of Marshall; LSG, left stellate ganglion; LSPV, left superior pulmonary vein; LV, left ventricle; OSA, obstructive sleep apnea; PA, pulmonary artery; SLGP, superior left ganglionated plexus.

Neural Activity of SLGP, LSG, and Left RSN

Figure 5 shows no significant differences in SLGP, LSG, or left RSN neural activity among the 3 groups at baseline. Repetitive obstructive respiratory events for 1 hour significantly increased the SLGP, LSG, and left RSN neural activity in the OSA group compared with the control group (all $P<0.05$).
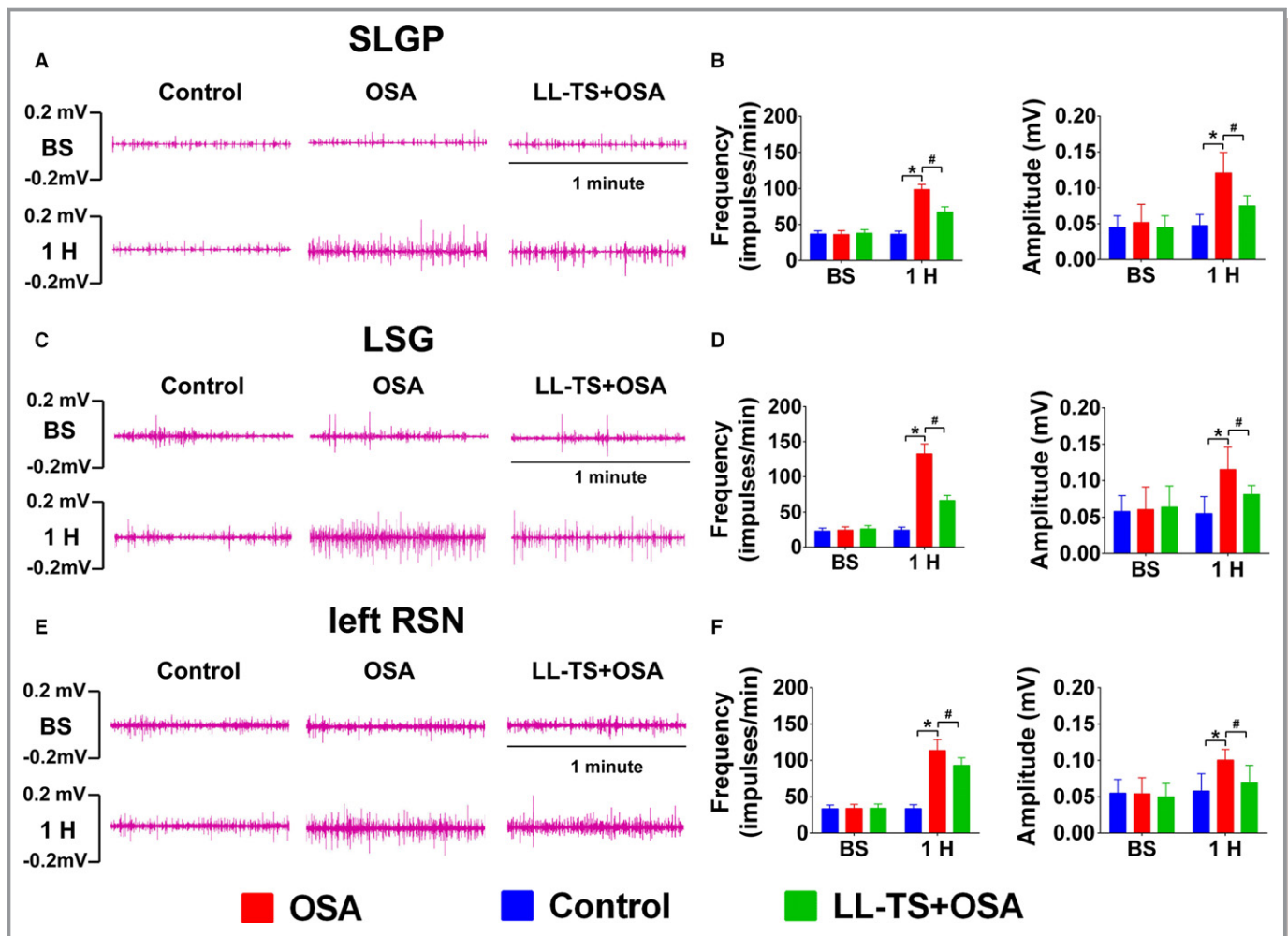
Figure 5. Autonomic neural activity changes in the control, OSA, and LL-TS + OSA groups. A, C, and E, Representative examples of the neural recordings from the SLGP, LSG and left RSN in different groups at baseline and 1 hour. B, D, and F, Quantitative analysis of autonomic neural activity in the SLGP, LSG, and left RSN (n=6). *$P<0.05$ vs the control group; #$P<0.05$ vs the OSA group. BS indicates baseline; LL-TS, low-level transcutaneous electrical stimulation; LSG, left stellate ganglion; OSA, obstructive sleep apnea; SLGP, superior left ganglionated plexus; RSN, renal sympathetic nerve.

However, the hyperactivity of SLGP, LSG, and left RSN was markedly inhibited in the LL-TS + OSA group compared with the OSA group (all $P<0.05$). For example, the neural activity of the LSG increased markedly in the OSA group compared with the control group (frequency: 24.50 ± 4.09 versus 132.83 ± 13.98 episodes/min; amplitude: 0.06 ± 0.02 versus 0.12 ± 0.03 mV; $P<0.05$). However, LL-TS significantly suppressed the OSA-induced enhanced neural activity of the LSG (frequency: 66.67 ± 7.15 episodes/min; amplitude: 0.08 ± 0.01 mV, $P<0.05$).

C-fos and NGF in the SLGP and the LSG

Figure 6 shows that the protein levels of c-fos and NGF in the SLGP and the LSG increased significantly in the OSA group compared with the control group (all $P<0.05$).

Immunofluorescence staining of the LSG in the OSA group revealed that the increased expression levels of c-fos and NGF were primarily localized in sympathetic neurons stained with tyrosine hydroxylase, which is a marker for sympathetic neurons. Quantitative data showed that c-fos- and NGF-positive sympathetic neurons in the OSA group were also significantly increased. However, these changes improved significantly in the LL-TS + OSA group compared with the OSA group (all $P<0.05$).

Discussion

This acute study of OSA-induced AF found that 1 hour of repetitive obstructive respiratory events significantly shortened the ERP and increased the ΣWOV on the atrium and pulmonary veins, which demonstrated that OSA facilitated AF
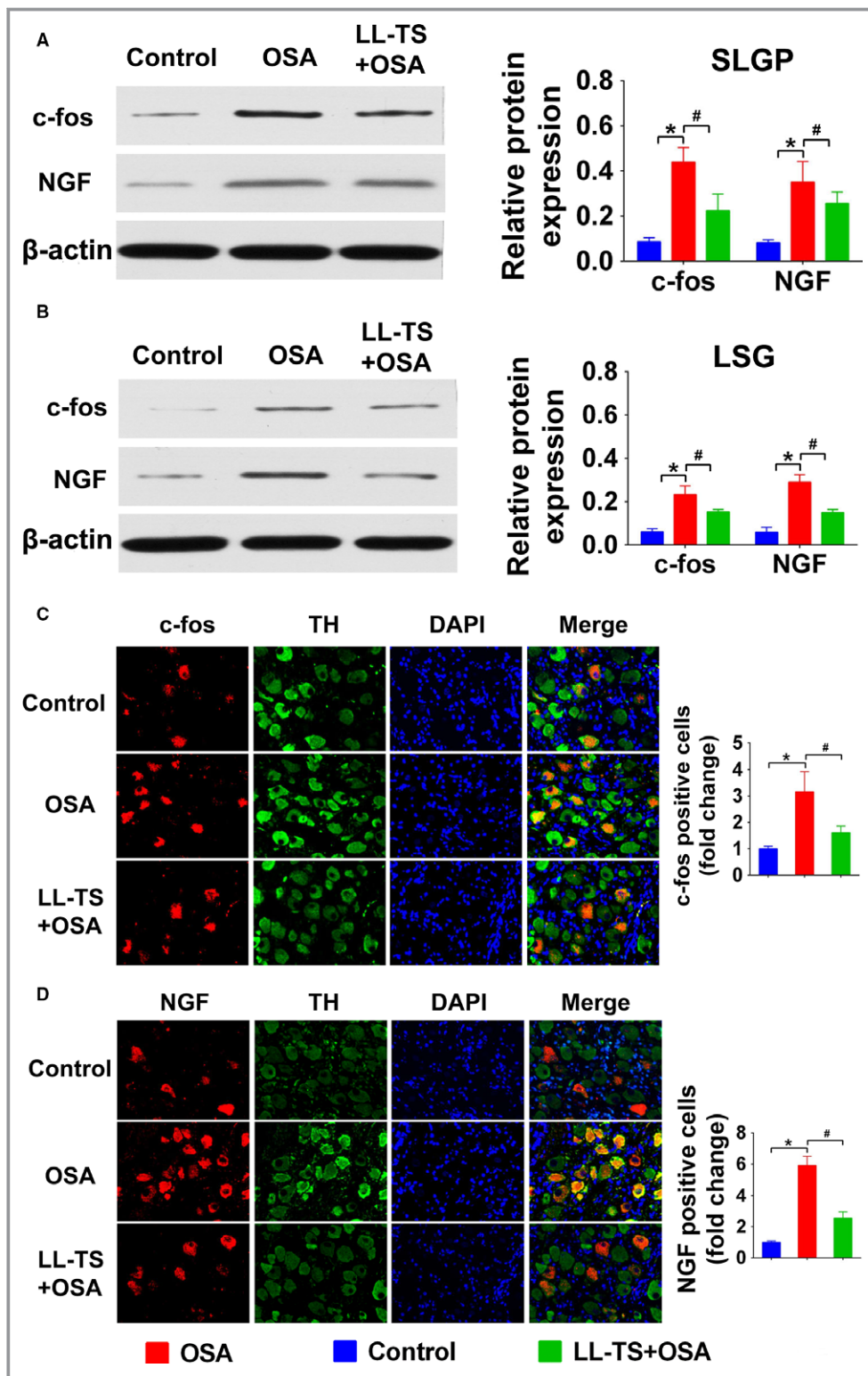
Figure 6. The expressions levels of c-fos and NGF in the control, OSA, and LL-TS + OSA groups. A and B, Representative examples and relative protein expression levels of c-fos and NGF in SLGP and LSG in the 3 groups (n=6). C and D, Representative photos and quantitative analyses of c-fos-immunoreactive and NGF-immunoreactive neurons in LSG (n=6). *P<0.05 vs the control group; #P<0.05 vs the OSA group. DAPI indicates 4′,6-diamidino-2-phenylindole; LL-TS, low-level transcutaneous electrical stimulation; LSG, left stellate ganglion; NGF, nerve growth factor; OSA, obstructive sleep apnea; SLGP, superior left ganglionated plexus; TH, tyrosine hydroxylase.

inducibility. Several lines of evidence indicated that the profibrillatory effects of OSA were mediated by hyperactivity of the intrinsic and extrinsic CANS. First, the frequency and amplitude of the neural activity directly recorded from the SLGP (the intrinsic CANS), the LSG (the extrinsic CANS), and the left RSN (the extrinsic CANS) were markedly upregulated after 1 hour of simulated OSA. Second, OSA also increased the SLGP and LSG functions. Third, our data showed that the c-fos and NGF expression levels in the SLGP and the LSG were markedly upregulated in the OSA group. Consequently, we suggested that hyperactivity of the intrinsic and extrinsic CANS plays crucial roles in the process of OSA-induced AF. Another major finding of this study was that noninvasive autonomic nervous modulation, LL-TS, significantly prolonged ERP at all sites and decreased the ΣWOV, the neural activity and function of the SLGP and the LSG, the neural activity of the left RSN, and the c-fos and NGF expression levels in the SLGP and the LSG. This suggested that LL-TS is an alternative noninvasive treatment for OSA-induced AF by effectively inhibiting the hyperactivity of the intrinsic and extrinsic CANS.

Autonomic Mechanism for AF Induced by OSA

Hypoxia and hypercapnia during OSA activate the autonomic nervous system via chemoreflexes.[25] Direct autonomic neural recording of the intrinsic CANS (including the SLGP and the ligament of Marshall) and extrinsic CANS (including LSG and vagal nerve activity) in an ambulatory canine model of intermittent rapid left atrial pacing showed that AF was preceded by the intrinsic CANS alone or coactivated with the extrinsic CANS.[26] Our recent study reported that 3 hours of RSN stimulation facilitated AF inducibility by upregulating CANS neural activity, including the SLGP and LSG.[16] Inhibition of the intrinsic and extrinsic CANS hyperactivity via ablation or electrical stimulation suppressed AF in different models,[5,17,24,27] which suggests that intrinsic and extrinsic CANS hyperactivity, including the SLGP, the LSG, and the RSN, plays important roles in the initiation and maintenance of AF. Numerous experimental studies have shown a strong association between the CANS and OSA-induced AF. Ghias et al[7] used direct autonomic neural recording and showed that the neural activity of the ganglionated plexi increased markedly
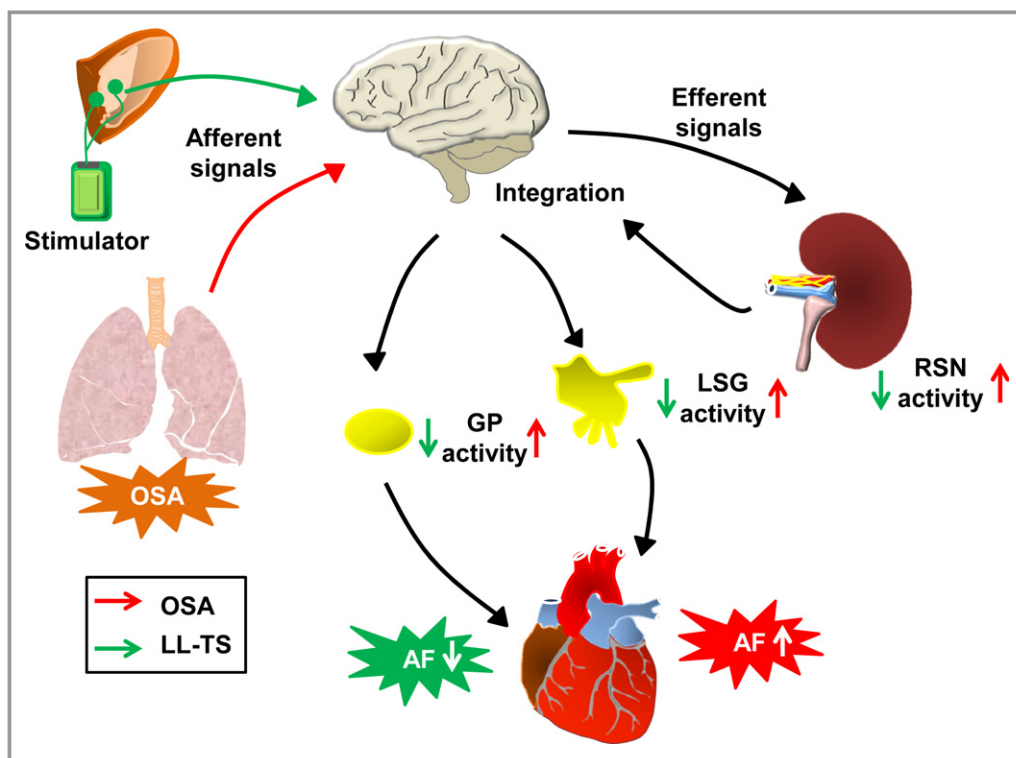

Figure 7. Schematic diagram illustrating how OSA initiates AF and the potential mechanism underlying the antiarrhythmic effect of LL-TS. OSA increases afferent signaling to the central nervous system, which integrates this information and leads to hyperactivity of the intrinsic and extrinsic cardiac autonomic nervous system, which increases the nerve activity of GP, LSG and RSN. Increased GP, LSG and RSN neural activities contribute to the initiation and maintenance of AF. However, LL-TS decreases input to the central nervous system and down-regulates the nerve activities of GP, LSG and RSN, which suppresses OSA-induced AF. AF indicates atrial fibrillation; GP, ganglionated plexus; LL-TS, low-level transcutaneous electrical stimulation; LSG, left stellate ganglion; OSA, obstructive sleep apnea; RSN, renal sympathetic nerve.

during the initiation of apnea-associated AF and that the ablation of ganglionated plexi significantly inhibited AF inducibility. Linz et al[5,10] demonstrated that renal denervation suppressed OSA-induced atrial ERP shortening and increased AF inducibility. Low-level baroreceptor stimulation, which also modulates autonomic balance, inhibited AF in a pig model of OSA.[9] These studies indicate that the modulation of autonomic remodeling inhibits OSA-induced AF inducibility. Our previous studies demonstrated that LL-TS reversed atrial remodeling and inhibited AF inducibility caused by rapid atrial pacing.[19,28] The present data showed that AF inducibility and the neural activity and function of the SLGP, the LSG, and the left RSN increased significantly during simulated OSA, consistent with previous studies. LL-TS significantly suppressed hyperactivity of the SLGP, the LSG, and the left RSN that was associated with low AF inducibility, which suggests that the intrinsic and extrinsic CANS contributes to the process of OSA-induced AF, and LL-TS suppresses OSA-induced AF by inhibiting intrinsic and extrinsic CANS hyperactivity.

Possible Mechanisms of Autonomic Remodeling of OSA-Induced AF

Previous studies demonstrated that a marker of fast neuron activation, c-fos, and a biomarker of growth, survival, and differentiation of sympathetic neurons, NGF, increased autonomic nervous system activity and facilitated the initiation of AF.[16,18,29] Our recent study reported that upregulation of c-fos and NGF expression levels in SLGP and LSG via RSN stimulation contributed to autonomic remodeling of the SLGP and the LSG and generated AF.[16] Wang et al[18] showed that the inhibition of c-fos and NGF expression levels in the anterior right ganglionated plexus. and the LSG suppressed autonomic remodeling and attenuated AF inducibility in a canine model of atrial rapid pacing. Chronic LL-TS reduced cardiac autonomic remodeling and attenuated cardiac arrhythmia inducibility by partially downregulating NGF expression in the LSG.[30] We found that simulated OSA significantly increased c-fos and NGF expression levels in hyperactive SLGP and LSG, which supports the finding that high expression levels of c-fos and NGF facilitated autonomic remodeling in OSA-induced AF. LL-TS significantly downregulated the expression levels of c-fos and NGF and inhibited the hyperactivity of the intrinsic and extrinsic CANS, which suggested that LL-TS suppressed autonomic remodeling by modulating c-fos and NGF expression.

Clinical Implications

Many clinical studies revealed that OSA was highly associated with AF. Mehra et al[31] reported that the risk of AF in patients with severe OSA was ≈4 times higher than that in patients without OSA. Another retrospective cohort study by Gami et al[32] found that the morbidity of new-onset AF in 3542 patients with OSA was 14%; therefore, OSA may be considered a univariate predictor of AF. OSA also partially counteracted the outcome of treatments for AF, such as radiofrequency catheter ablation[33] and drugs.[34] However, the first-line therapy of OSA, continuous positive airway pressure ventilation, has shown relatively low compliance in patients with OSA.[35] Novel optional therapies are needed to prevent and treat AF in OSA patients. LL-TS inhibited OSA-induced AF without surgical intervention in the present study. LL-TS also suppressed AF in patients with paroxysmal AF.[36] Consequently, we suggest that LL-TS is a novel therapy for OSA-induced AF.

Study Limitations

Several limitations maybe noted in this study. First, the dogs maintained a left lateral position throughout the experiment, and we selected the SLGP, LSG, and left RSN to represent the intrinsic and extrinsic CANS to stably measure repetitive electrophysiological and CANS-related data. Second, anesthesia with pentobarbital activates the autonomic nervous system,[19] but animals in the control, OSA, and LL-TS + OSA groups all received similar anesthesia, which should mitigate the effect of anesthesia on the neural activity of the autonomic nervous system among these groups. Third, we performed only 1-hour OSA and 1-hour LL-TS in this study, so long-term effects of LL-TS on chronic OSA should be further investigated.

Conclusion

The intrinsic and extrinsic CANS plays crucial roles during the acute stage of shortening of atrial refractoriness and OSA-induced AF (Figure 7). LL-TS suppressed shortening of atrial refractoriness and autonomic remodeling and protected against OSA-induced AF.

Sources of Funding

Disclosures

None.

References

1. Tilkian AG, Guilleminault C, Schroeder JS, Lehrman KL, Simmons FB, Dement WC. Sleep-induced apnea syndrome. Prevalence of cardiac arrhythmias and their reversal after tracheostomy. *Am J Med*. 1977;63:348–358.

2. Guilleminault C, Connolly SJ, Winkle RA. Cardiac arrhythmia and conduction disturbances during sleep in 400 patients with sleep apnea syndrome. *Am J Cardiol*. 1983;52:490–494.

3. Zhang L, Hou Y, Po SS. Obstructive sleep apnoea and atrial fibrillation. *Arrhythm Electrophysiol Rev*. 2015;4:14–18.

4. Linz D, Linz B, Hohl M, Bohm M. Atrial arrhythmogenesis in obstructive sleep apnea: therapeutic implications. *Sleep Med Rev*. 2016;26:87–94.

5. Linz D, Mahfoud F, Schotten U, Ukena C, Neuberger HR, Wirth K, Bohm M. Renal sympathetic denervation suppresses postapneic blood pressure rises and atrial fibrillation in a model for sleep apnea. *Hypertension*. 2012;60:172–178.

6. Schotten U, Verheule S, Kirchhof P, Goette A. Pathophysiological mechanisms of atrial fibrillation: a translational appraisal. *Physiol Rev*. 2011;91:265–325.

7. Ghias M, Scherlag BJ, Lu Z, Niu G, Moers A, Jackman WM, Lazzara R, Po SS. The role of ganglionated plexi in apnea-related atrial fibrillation. *J Am Coll Cardiol*. 2009;54:2075–2083.

8. Gao M, Zhang L, Scherlag BJ, Huang B, Stavrakis S, Hou YM, Hou Y, Po SS. Low-level vagosympathetic trunk stimulation inhibits atrial fibrillation in a rabbit model of obstructive sleep apnea. *Heart Rhythm*. 2015;12:818–824.

9. Linz D, Hohl M, Khoshkish S, Mahfoud F, Ukena C, Neuberger HR, Wirth K, Bohm M. Low-level but not high-level baroreceptor stimulation inhibits atrial fibrillation in a pig model of sleep apnea. *J Cardiovasc Electrophysiol*. 2016;27:1086–1092.

10. Linz D, Hohl M, Nickel A, Mahfoud F, Wagner M, Ewen S, Schotten U, Maack C, Wirth K, Bohm M. Effect of renal denervation on neurohumoral activation triggering atrial fibrillation in obstructive sleep apnea. *Hypertension*. 2013;62:767–774.

11. Jordan AS, McSharry DG, Malhotra A. Adult obstructive sleep apnoea. *Lancet*. 2014;383:736–747.

12. Roche F, Xuong AN, Court-Fortune I, Costes F, Pichot V, Duverney D, Vergnon JM, Gaspoz JM, Barthelemy JC. Relationship among the severity of sleep apnea syndrome, cardiac arrhythmias, and autonomic imbalance. *Pacing Clin Electrophysiol*. 2003;26:669–677.

13. Gami AS, Somers VK. Implications of obstructive sleep apnea for atrial fibrillation and sudden cardiac death. *J Cardiovasc Electrophysiol*. 2008;19:997–1003.

14. Randall WC. Changing perspectives concerning neural control of the heart. In: Armour JA, Ardell JL, eds. *Neurocardiology. Chapter 1*. New York, NY: Oxford University Press; 1994.

15. Ardell JL. Structure and function of the mammalian intrinsic cardiac neurons. In: Armour JA, Ardell JL, eds. *Neurocardiology. Chapter 5*. New York, NY: Oxford University Press; 1994.

16. Yu L, Huang B, Wang Z, Wang S, Wang M, Li X, Zhou L, Meng G, Yuan S, Zhou X, Jiang H. Impacts of renal sympathetic activation on atrial fibrillation: the potential role of the autonomic cross talk between kidney and heart. *J Am Heart Assoc*. 2017;6:e004716. DOI: 10.1161/JAHA.116.004716.

17. Tan AY, Zhou S, Ogawa M, Song J, Chu M, Li H, Fishbein MC, Lin SF, Chen LS, Chen PS. Neural mechanisms of paroxysmal atrial fibrillation and paroxysmal atrial tachycardia in ambulatory canines. *Circulation*. 2008;118:916–925.

18. Wang S, Zhou X, Huang B, Wang Z, Zhou L, Chen M, Yu L, Jiang H. Spinal cord stimulation suppresses atrial fibrillation by inhibiting autonomic remodeling. *Heart Rhythm*. 2016;13:274–281.

19. Yu L, Scherlag BJ, Li S, Fan Y, Dyer J, Male S, Varma V, Sha Y, Stavrakis S, Po SS. Low-level transcutaneous electrical stimulation of the auricular branch of the vagus nerve: a noninvasive approach to treat the initial phase of atrial fibrillation. *Heart Rhythm*. 2013;10:428–435.

20. Wang Z, Yu L, Wang S, Huang B, Liao K, Saren G, Tan T, Jiang H. Chronic intermittent low-level transcutaneous electrical stimulation of auricular branch of vagus nerve improves left ventricular remodeling in conscious dogs with healed myocardial infarction. *Circ Heart Fail*. 2014;7:1014–1021.

21. Sheng X, Scherlag BJ, Yu L, Li S, Ali R, Zhang Y, Fu G, Nakagawa H, Jackman WM, Lazzara R, Po SS. Prevention and reversal of atrial fibrillation inducibility and autonomic remodeling by low-level vagosympathetic nerve stimulation. *J Am Coll Cardiol*. 2011;57:563–571.

22. Wei SG, Felder RB. Forebrain renin-angiotensin system has a tonic excitatory influence on renal sympathetic nerve activity. *Am J Physiol Heart Circ Physiol*. 2002;282:H890–H895.

23. Nakamura T, Kawahara K, Kusunoki M, Feng Z. Microneurography in anesthetized rats for the measurement of sympathetic nerve activity in the sciatic nerve. *J Neurosci Methods*. 2003;131:35–39.

24. Yu L, Scherlag BJ, Li S, Sheng X, Lu Z, Nakagawa H, Zhang Y, Jackman WM, Lazzara R, Jiang H, Po SS. Low-level vagosympathetic nerve stimulation inhibits atrial fibrillation inducibility: direct evidence by neural recordings from intrinsic cardiac ganglia. *J Cardiovasc Electrophysiol*. 2011;22:455–463.

25. Olson LJ, Somers VK. Chemoreflexes, sympathetic excitation, and heart failure-challenges and opportunities. *J Card Fail*. 2013;19:416–418.

26. Choi EK, Shen MJ, Han S, Kim D, Hwang S, Sayfo S, Piccirillo G, Frick K, Fishbein MC, Hwang C, Lin SF, Chen PS. Intrinsic cardiac nerve activity and paroxysmal atrial tachyarrhythmia in ambulatory dogs. *Circulation*. 2010;121:2615–2623.

27. Lu Z, Scherlag BJ, Lin J, Niu G, Fung KM, Zhao L, Ghias M, Jackman WM, Lazzara R, Jiang H, Po SS. Atrial fibrillation begets atrial fibrillation: autonomic mechanism for atrial electrical remodeling induced by short-term rapid atrial pacing. *Circ Arrhythm Electrophysiol*. 2008;1:184–192.

28. Chen M, Zhou X, Liu Q, Sheng X, Yu L, Wang Z, Wang S, Zhou S. Left-sided noninvasive vagus nerve stimulation suppresses atrial fibrillation by upregu-lating atrial gap junctions in canines. *J Cardiovasc Pharmacol*. 2015;66:593–599.

29. Linz D, van Hunnik A, Hohl M, Mahfoud F, Wolf M, Neuberger HR, Casadei B, Reilly SN, Verheule S, Bohm M, Schotten U. Catheter-based renal denervation reduces atrial nerve sprouting and complexity of atrial fibrillation in goats. *Circ Arrhythm Electrophysiol*. 2015;8:466–474.

30. Yu L, Wang S, Zhou X, Wang Z, Huang B, Liao K, Saren G, Chen M, Po SS, Jiang H. Chronic intermittent low-level stimulation of trgus reduces cardiac autonomic remodeling and ventricular arrhythmia inducibility in a post-infarction canine model. *JACC Clin Electrophysiol*. 2016;2:330–339.

31. Mehra R, Benjamin EJ, Shahar E, Gottlieb DJ, Nawabit R, Kirchner HL, Sahadevan J, Redline S; Sleep Heart Health S. Association of nocturnal arrhythmias with sleep-disordered breathing: the Sleep Heart Health Study. *Am J Respir Crit Care Med*. 2006;173:910–916.

32. Gami AS, Hodge DO, Herges RM, Olson EJ, Nykodym J, Kara T, Somers VK. Obstructive sleep apnea, obesity, and the risk of incident atrial fibrillation. *J Am Coll Cardiol*. 2007;49:565–571.

33. Ng CY, Liu T, Shehata M, Stevens S, Chugh SS, Wang X. Meta-analysis of obstructive sleep apnea as predictor of atrial fibrillation recurrence after catheter ablation. *Am J Cardiol*. 2011;108:47–51.

34. Monahan K, Brewster J, Wang L, Parvez B, Goyal S, Roden DM, Darbar D. Relation of the severity of obstructive sleep apnea in response to anti-arrhythmic drugs in patients with atrial fibrillation or atrial flutter. *Am J Cardiol*. 2012;110:369–372.

35. McArdle N, Devereux G, Heidarnejad H, Engleman HM, Mackay TW, Douglas NJ. Long-term use of CPAP therapy for sleep apnea/hypopnea syndrome. *Am J Respir Crit Care Med*. 1999;159:1108–1114.

36. Stavrakis S, Humphrey MB, Scherlag BJ, Hu Y, Jackman WM, Nakagawa H, Lockwood D, Lazzara R, Po SS. Low-level transcutaneous electrical vagus nerve stimulation suppresses atrial fibrillation. *J Am Coll Cardiol*. 2015;65:867–875.